

Modelling an Artificial Microalgae-Cyanobacteria Ecosystem

Margaux Caïa, Olivier Bernard, Jean-Philippe Steyer

▶ **To cite this version:**

Margaux Caïa, Olivier Bernard, Jean-Philippe Steyer. Modelling an Artificial Microalgae-Cyanobacteria Ecosystem. IFAC-PapersOnLine, 2018, 51 (2), pp.655 - 660. ⟨10.1016/j.ifacol.2018.03.111⟩. ⟨hal-01833296⟩

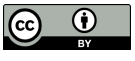
HAL Id: hal-01833296

https://hal.sorbonne-universite.fr/hal-01833296v1

Submitted on 9 Jul 2018

HAL is a multi-disciplinary open access archive for the deposit and dissemination of scientific research documents, whether they are published or not. The documents may come from teaching and research institutions in France or abroad, or from public or private research centers.

L'archive ouverte pluridisciplinaire **HAL**, est destinée au dépôt et à la diffusion de documents scientifiques de niveau recherche, publiés ou non, émanant des établissements d'enseignement et de recherche français ou étrangers, des laboratoires publics ou privés.



Distributed under a Creative Commons CC BY 4.0 - Attribution - International License

Available online at www.sciencedirect.com

ScienceDirect

IFAC Papers Online CONFERENCE PAPER ARCHIVE

IFAC PapersOnLine 51-2 (2018) 655–660

Modelling an Artificial Microalgae-Cyanobacteria Ecosystem

Margaux Caia *,**,***,1 **Olivier Bernard** **,***
Jean-Philippe Steyer *

* *LBE, Univ. Montpellier, INRA, Narbonne, France*
** *Univ. Nice Côte d'Azur, INRIA BIOCORE, 06902 Sophia Antipolis, France*
*** *Sorbonne Universités, UPMC, INSU-CNRS, Laboratoire d'Océanographie de Villefranche, 06230 Villefranche-sur-Mer, France*

Abstract: Microalgae based processes have been actively studied in the last decades with perspective for food, feed, and source of chemicals such as biofuels. Most of the developments focused on monospecific culture of microalgae, with dedicated practices to avoid any contaminations. However, interactions between microalgae and bacteria are likely to enhance microalgae growth, provide more resilience to external changes and eventually limit external contaminations. But interactions within these natural ecosystems are still poorly understood and are affected by the environment. A photosynthetic marine ecosystem composed of the microalgae *Dunaliella salina* and the nitrogen fixing cyanobacteria *Crocosphaera watsonii* was therefore studied. A model was designed to represent the competition for light and the interactions with nitrogen between these two microorganisms. An allelopathic effect was noticed and a toxin production by *C. watsonii* was assumed and included in the model. Calibration was carried out with experimental data where cell densities and nitrate concentrations were measured. The predictions of the mathematical model accurately represented the experimental data. The model therefore highlighted the interactions within this artificial ecosystem. The model confirms that *D. salina* growth was limited by nitrate concentration and did not consume dissolved organic nitrogen produced by *C. watsonii* from its diazotrophic activity. *D. salina* and *C. watsonii* were competing for light, which favored *D. salina* and limited *C. watsonii* when grown in cocultures. The model supports the hypothesis that *C. watsonii* produced toxins enhancing *D. salina* mortality in the cocultures.

© 2018, IFAC (International Federation of Automatic Control) Hosting by Elsevier Ltd. All rights reserved.

Keywords: Interactions, Environmental engineering, Ecology, Modelling, Biotechnology, *Crocosphaera watsonii*, *Dunaliella salina*, Diazotrophy, Nitrogen fixation, Allelopathy.

1. INTRODUCTION

Photosynthetic microalgae are part of the phytoplankton and play a major part in the biogeochemical cycles of the ocean (Minowa and Sawayama, 1999). Microalgae have attracted much interests in the last decade because of their potential to produce, at a high rate and with limited environmental impact, lipids, proteins, antioxidant or pigments which can be used in different industries (Barra et al., 2014). Most of the processes use monospecific microalgae at a high cost to limit external contaminations. However, symbiotic cultures with bacteria or cyanobacteria are likely to enhance microalgae growth, provide more resilience to external changes and eventually limit external contaminations (Le Chevanton et al., 2013). In particular, growing simultaneously microalgae with nitrogen fixing cyanobacteria has been described as a promising way to support the nitrogen need of microalgae (Do Nascimento et al., 2015).

Interactions between microalgae, cyanobacteria and bacteria are still poorly understood (Fouilland, 2012; Fuentes et al., 2016). Interactions between the different organisms can either be positive, negative or neutral (Ramanan et al., 2016). Interactions between algae and bacteria are affected by environmental parameters such as pH, CO_2 and nitrogen source and concentration (Huisman et al., 1999; Le Chevanton et al., 2013; Ying et al., 2014). An artificial ecosystem composed of algae and bacteria is likely to be more resistant to variations in temperature and medium composition and to limit external contaminations by occupying all the ecological niches (Fouilland, 2012).

No living eukaryotic organism is known to uptake atmospheric N_2 as a source of nitrogen whereas it is the principal pathway for nitrogen acquisition in diazotrophic cyanobacteria (Thompson et al., 2012). In particular, the unicellular cyanobacterium *Crocosphaera watsonii* is known for its high diazotrophic activity. The idea that we explore here is to assemble these cyanobacteria together with *Dunaliella salina*, a microalgae of commercial interest. The N_2 uptaken and partially released in the form of organic dissolved nitrogen (Berthelot et al., 2015, 2016) is therefore expected to be used as a nitrogen substrate by *D. salina*. No negative interactions between cyanobacteria

[1] Corresponding author, email: margaux.caia@inra.fr

2405-8963 © 2018, IFAC (International Federation of Automatic Control) Hosting by Elsevier Ltd. All rights reserved.
Peer review under responsibility of International Federation of Automatic Control.
10.1016/j.ifacol.2018.03.111

and microalgae have been described (Olli et al., 2015) but both *D. salina* and *C. watsonii* use light for photosynthesis. A competition for light is thus expected.

The objective of this work was therefore to assess the main interactions within an artificial ecosystem composed of *D. salina* and *C. watsonii*. A mathematical model was built to support the hypotheses on the interactions and quantify their impacts on overall productivity.

The paper first rapidly presents the experimental material and methods. The ecosystem model is then presented and calibrated. Simulations are then analysed to assess the potential of this ecosystem.

2. MATERIAL AND METHODS

2.1 Experimental settings

Medium culture. Seawater was filtered on 0.1 μm. F/2 nutrients were added by filtration to the previously autoclaved filtered seawater (Guillard, 1975).

Monocultures and cocultures of C. watsonii and D. salina. Two monocultures and one coculture of *C. watsonii* and *D. salina* were cultivated in triplicates in batch in 250 mL Erlenmeyers. Non-axenic strains of *C. watsonii* WH8501 and *D. salina* CCAP19/18 were inoculated from cultures kept in exponential growth phase in order to obtain a cellular concentration of respectively 1.10^9 and 4.10^7 cell.L^{-1} to ensure an adequate cyanobacteria/microalgae ratio through the experiment. The cultures were kept in an incubator (SANYO MLR-351, Japan) at 27°C, and at a light intensity of 220 μmol photons.m^{-2}.s^{-1} with a day/night cycle of 12h:12h. 0.2 μm filtered air was bubbled constantly in the agitated cultures.

2.2 Measurements

Cell counts and growth rates. Cell counts were performed with a Coulter Counter (Multisizer III; Beckman-Coulter) to follow both cyanobacteria and microalgae growths. *C. watsonii* and *D. salina* can be numbered easily because of their different diameter size (respectively 1.5-3 μm and 7-13 μm).

The growth rate was calculated during the exponential growth phase. Each cell count was converted into its neperian logarithm. A linear regression was performed on the neperian logarithms. The growth rate corresponded to the slope of the line.

Nitrate. Nitrate (NO_3^-) concentration was measured to follow the microalgae consumption. Cultures samples were filtered with 0.2 μm pore diameters syringe-filters to eliminate cellular biomass and were then analyzed with an Auto-analyser II Technicon.

Dissolved organic nitrogen measurement. Cultures were filtered with 0.2 μm pore diameters syringe-filters. Dissolved Organic Nitrogen (DON) concentration was measured according to the wet-oxydation protocol from Pujo-Pay and Raimbault (1994) with an Auto-analyser II Technicon.

Light intensity. The light intensity received by the cultures vary depending on the Erlenmeyers position because of their proximity to the neons in the incubator. The light intensity was measured at the center of the cultures each morning with a Quantameter (PAR Sensor QSL-2100, Biospherical Instruments).

3. MODEL DESIGN

3.1 Light intensity along the reactor

Cultures were lightened on their external sides with a constant light intensity I_0. The light intensity I_0 was constant from 8 am until 8 pm and was equal to 220 μmol photons.m^{-2}.s^{-1}. The rest of the day was a night period, and light intensity I_0 was 0 μmol photons.m^{-2}.s^{-1}. The self-shading by the microalgae and cyanobacteria was considered, assuming that both species contribute to attenuate light. Light is attenuated due to absorption and scattering, depending on cell concentrations, size and pigment content.

$$I = I_0 \mathrm{e}^{-K(X)L} \tag{1}$$

where I is the light intensity at the center of the Erlenmeyer, assuming an optical path L between the external surface and the core of the Erlenmeyer (m). $K(X)$ is the extinction coefficient (m^2.cell^{-1}) depending on X, the concentration vector of the two biomasses.

Light attenuation characteristics are specific to each species and are represented in (2) as the extinction coefficient K_{ext}. The overall attenuation coefficient $K(X)$ is assumed to be the sum of the attenuations due to each species. D and C denote respectively *D. salina* and *C. watsonii* algal concentrations (cell.m^{-3}). $K_{\mathrm{ext,d}}$ and $K_{\mathrm{ext,c}}$ are respectively *D. salina* and *C. watsonii* light extinction coefficients (m^2.cell^{-1}), so that $K(X) = K_{\mathrm{ext,d}}D + K_{\mathrm{ext,c}}C$ in cocultures.

Average light intensity within the culture medium $\overline{I}$ was considered to drive photosynthesis.

$$\overline{I} = \frac{I_0}{L} \frac{1-\mathrm{e}^{-(K_{\mathrm{ext,d}}D+K_{\mathrm{ext,c}}C)L}}{K_{\mathrm{ext,d}}D + K_{\mathrm{ext,c}}C} \tag{2}$$

3.2 Growth and substrate uptake

C. watsonii growth rate is assumed to depend on the light intensity $\overline{I}$ with a simple Michaelis-Menten kinetics (Grimaud et al., 2014). The respiration rate was also considered. *C. watsonii* growth can therefore be represented by following dynamics:

$$\frac{dC}{dt} = \overline{\mu_{\mathrm{c}}} \frac{\overline{I}}{\overline{I}+K_{\mathrm{I,c}}} C - R_{\mathrm{c}}C - \upsilon C \tag{3}$$

where $\overline{\mu_{\mathrm{c}}}$ is the maximum growth rate (d^{-1}), $K_{\mathrm{I,c}}$ is the half-saturation constant for light (μmol photons.m^{-2}.s^{-1}), and R_{c} is the respiration rate (d^{-1}). Finally, υ is the dilution rate of the reactor (d^{-1}).

Cyanobacteria are known to produce cyanotoxins in presence of a competitor but nothing is known about a potential production by *C. watsonii* (Dunker et al., 2017). In order to fit experimental observations, we assume here

that *C. watsonii* produces a nitrogen rich inhibiting compound P (mol.L^{-1}), proportionally to the cyanobacteria cell concentration:

$$\frac{dP}{dt} = \alpha C - \upsilon P \quad (4)$$

where α is the toxin production rate (mol.cell^{-1}.d^{-1}).

For the microalgae *D. salina*, we follow Droop's theory and we assume that growth depends on internal nitrogen quota and on light intensity (Bernard, 2011). We also consider that cell mortality is induced by the compound P produced by *C. watsonii*. Finally, the resulting dynamics is:

$$\frac{dD}{dt} = \overline{\mu_{\mathrm{d}}}(1-\frac{Q_0}{Q})\frac{\overline{I}}{\overline{I}+K_{\mathrm{I,d}}}D - R_{\mathrm{d}}D - m\frac{P}{P+K_{\mathrm{P}}D} - \upsilon D \quad (5)$$

where $\overline{\mu_{\mathrm{d}}}$ is the growth rate at infinite nitrogen quota (d^{-1}), Q is the intracellular nitrogen quota and Q_0 is the minimum intracellular nitrogen quota (mol N.cell^{-1}), R_{d} is the respiration rate (d^{-1}), $K_{\mathrm{I,d}}$ is the half-saturation constant for light (μmol photons.m^{-2}.s^{-1}), m is the maximum mortality rate (d^{-1}), and K_{P} is the half-saturation constant for *C. watsonii* potential toxins (mol P.L^{-1}).

The nitrogen concentration (mol N.L^{-1}), denoted S, results from the balance between nitrogen supply at concentration S_{in} and uptake by *D. salina* (*C. watsonii* does not consume any nitrate). We use the expression proposed by Bougaran et al. (2010) to account for the downregulation of nitrogen uptake for high nitrogen quota. Finally, equation 6 represents the inorganic nitrogen dynamics:

$$\frac{dS}{dt} = -\rho_{\mathrm{m}}\frac{S}{S+K_{\mathrm{S}}}(\frac{Q_{\mathrm{L}}-Q}{Q_{\mathrm{L}}-Q_0})D + \upsilon S_{\mathrm{in}} - \upsilon D \quad (6)$$

where ρ_{m} is *D. salina* maximum rate of nitrogen acquisition (mol N.cell^{-1}.d^{-1}), K_{S} is the half-saturation constant for nitrogen (mol.L^{-1}), and Q_{L} is the intracellular nitrogen quota for which nitrogen uptake stops (mol N.cell^{-1}).

The dynamics of the nitrogen quota for *D. salina* result from nitrogen uptake and dilution by cell growth. The quota dynamics are therefore determined as follows:

$$\frac{dQ}{dt} = \rho_{\mathrm{m}}\frac{S}{S+K_{\mathrm{S}}}(\frac{Q_{\mathrm{L}}-Q}{Q_{\mathrm{L}}-Q_0}) - \overline{\mu_{\mathrm{d}}}(1-\frac{Q_0}{Q})\frac{\overline{I}}{\overline{I}+K_{\mathrm{I,d}}}Q \quad (7)$$

3.3 Model calibration

C. watsonii. The net growth rate μ_{net} and half-saturation constant for light for *C. watsonii* were reported from Goebel et al. (2008). The maximum growth rate and respiration rate were calculated from preliminary *C. watsonii* monoculture experiments under various lights as follows:

$$\begin{cases} \overline{\mu_{\mathrm{c}}} = \mu_{\mathrm{net}} + R_{\mathrm{c}} \\ R_{\mathrm{c}} = \overline{\mu_{\mathrm{c}}}\dfrac{I_{\mathrm{x,c}}}{I_{\mathrm{x,c}}+K_{\mathrm{I,c}}} - \mu_{\mathrm{x,c}} \end{cases} \quad (8)$$

where $\mu_{\mathrm{x,c}}$ is the experimental growth rate (d^{-1}), and $I_{\mathrm{x,c}}$ is the average experimental light intensity measured during the exponential growth phase (μmol photons.m^{-2}.s^{-1}).

D. salina. The respiration rate and half-saturation coefficient for nitrogen were reported from Fachet et al. (2014) whereas the nitrogen acquisition rate was reported from Bonnefond et al. (2016). The growth rate at infinite nitrogen quota and half-saturation constant for light of *D. salina* were determined from preliminary monoculture experiments of *D. salina* where the growth rate was measured for various light intensities, as described in Section 2.2. The two parameters were thus computed to fit these experimental data, by considering the linear regression between $1/(\mu_{\mathrm{x,d}}+R_{\mathrm{d}})$ and $1/\bar{I}$ (9) to calculate *D. salina* maximum growth rate and half-saturation constant for light as follows:

$$\frac{1}{\mu_{\mathrm{x,d}}+R_{\mathrm{d}}} = \frac{K_{\mathrm{I,d}}}{\overline{\mu_{\mathrm{d}}}}\frac{Q_{\max}}{Q_{\max}-Q_{\min}}\frac{1}{I_{\mathrm{x,d}}} + \frac{1}{\overline{\mu_{\mathrm{d}}}}\frac{Q_{\max}}{Q_{\max}-Q_{\min}} \quad (9)$$

where $\mu_{\mathrm{x,d}}$ is the experimental growth rate (d^{-1}), $I_{\mathrm{x,d}}$ is the average experimental light intensity measured during the exponential growth phase (μmol photons.m^{-2}.s^{-1}), and $Q_{\max}$ and $Q_{\min}$ are respectively the maximum and minimum nitrogen cellular quota (mol N.cell^{-1}). The calculated $\overline{\mu_{\mathrm{d}}}$ was doubled in order to fit the day/night cycle and reach the appropriate average growth rate in 24h.

Other parameters estimations. The light extinction coefficients were estimated from preliminary *D. salina* and *C. watsonii* monocultures experiments to make the model fit the data. The minimal and maximal nitrogen intracellular quota were obtained from simulations of preliminary experiments. However, the toxin production rate by *C. watsonii*, the half-saturation constant for toxin and mortality rate for *D. salina* were estimated from the cocultures experimental data since nothing is known about the toxin productivity and impact.

Table 1. Parameters list (obtained from (a): preliminary experiments; (b): bibliography; (c): fitting)

Parameter		Value and unit	Source
$\overline{\mu_{\mathrm{c}}}$	Growth rate	0.58 d^{-1}	(a,b)
$K_{\mathrm{I,c}}$	Half-saturation constant for I	57 μmol photons. m^{-2}.s^{-1}	(b)
R_{c}	Respiration rate	9·10^{-2} d^{-1}	(a,b)
α	Toxin production rate	1·10^{-4} mol.cell^{-1}	(c)
$K_{\mathrm{ext,c}}$	Light extinction coefficient	1·10^{-10} m^2.cell^{-1}	(a)
$\overline{\mu_{\mathrm{d}}}$	Growth rate	4.99 d^{-1}	(a)
$K_{\mathrm{I,d}}$	Half-saturation constant for I	154 μmol photons. m^{-2}.s^{-1}	(a)
R_{d}	Respiration rate	0.16 mol.d^{-1}	(b)
$K_{\mathrm{ext,d}}$	Light extinction coefficient	2.3·10^{-9} m^2.cell^{-1}	(a)
K_{P}	Half-saturation constant for toxins	5·10^{-2} mol P.m^{-3}	(c)
m	Mortality rate	3.4·10^{-2} d^{-1}	(c)
ρ_{m}	Nitrogen acquisition rate	9.8·10^{-7} mol N.cell^{-1}.d^{-1}	(b)
K_{S}	Half-saturation constant for N	1.1·10^{-2} mol N.m^{-3}	(b)
$Q_{\max}$	Maximum N cellular quota	1.3·10^{-6} mol N.cell^{-1}	(a)
$Q_{\min}$	Minimum N cellular quota	5.4·10^{-7} mol N.cell^{-1}	(a)

4. SIMULATION OF THE INTERACTIONS BETWEEN *D. SALINA* AND *C. WATSONII*

The model was validated with data not used for calibration and accurately represents both cellular growth and nitro-

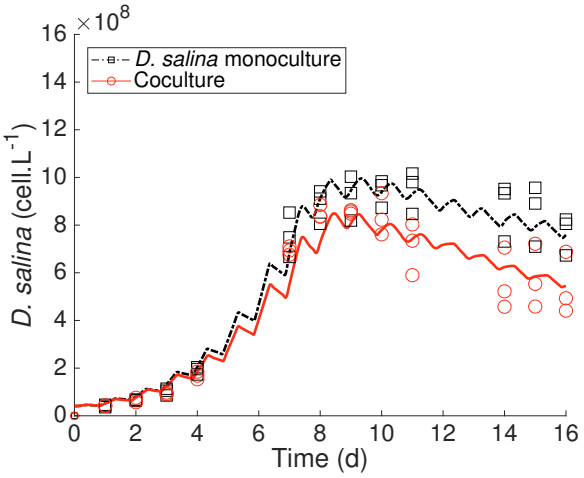


Fig. 1. *D. salina* in monocultures and cocultures (lines: theoretical data, symbols: experimental data)

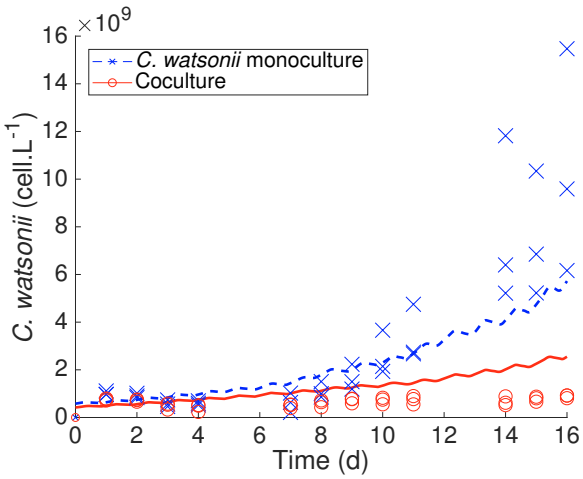


Fig. 2. *C. watsonii* in monocultures and cocultures (lines: theoretical data, symbols: experimental data)

gen consumption for the two microorganisms in monocultures. *D. salina* exponential growth phase slows down when nitrate is consumed and eventually stops (Figures 1 and 3). NO_3^- is therefore limiting growth. The dynamics are very different for the diazotrophic cyanobacterium *C. watsonii* which only uses atmospheric N_2 (Dron et al., 2012) as nitrogen source. *C. watsonii* growth never stops, but is progressively reduced by the lower light, while nitrate is never consumed (Figures 2 and 3).

An amount of 105±32 μmol.L^{-1} of Dissolved Organic Nitrogen (DON) is measured into *C. watsonii* monocultures, as a by-product of diazotrophic fixation whereas 6.4±28 μmol.L^{-1} DON are measured in the cocultures. *D. salina* maximal cell concentration is not higher when cocultivated and is eventually limited by NO_3^- as in the monocultures (Figures 1 and 3). *D. salina* therefore do not consume the DON produced by *C. watsonii* in the cocultures. The lower DON might result from the lower biomass (and diazotrophic activity) when *C. watsonii* is cocultivated. This result is consistent with the pattern of the hypothesized compound P, which is 2.7 times lower in coculture than in monoculture. However, the difference between the model and the cultures could be explained by a DON consumption by bacteria since the cultures were not axenic.

C. watsonii growth is significantly reduced in the cocultures whereas *D. salina* exponential growth phase is only marginally affected as shown in Figures 1 and 2. The microalgae and the cyanobacteria are not in competition for nutrients, and it results that *C. watsonii* still grow in cocultures, at a reduced rate, at the end of the experiment (Figure 2).

Light attenuation is mostly due to *D. salina* biomass accumulation (Figures 1 and 4). This light attenuation rapidly shadows *C. watsonii* which requires light in order to support both growth during the day and nitrogen fixation activity during the night. There is therefore a competition for light between the microalgae and the cyanobacteria (Huisman et al., 1999) which favors *D. salina* (Figure 4). This light competition is correctly represented by the model which also accurately simulates the day/night cycle of 12h:12h, as shown in Figure 4.

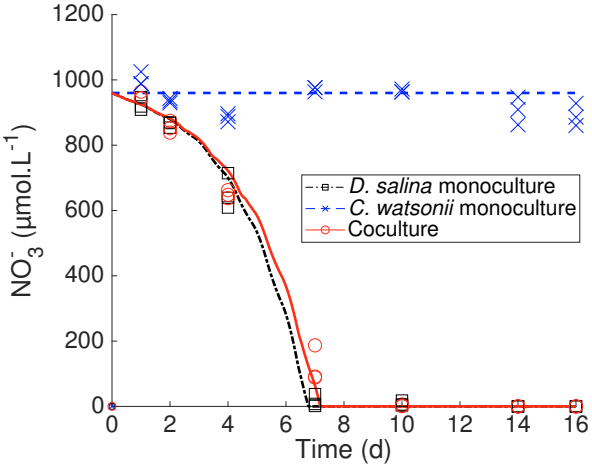


Fig. 3. Nitrate in monocultures and cocultures (lines: theoretical data, symbols: experimental data)

.

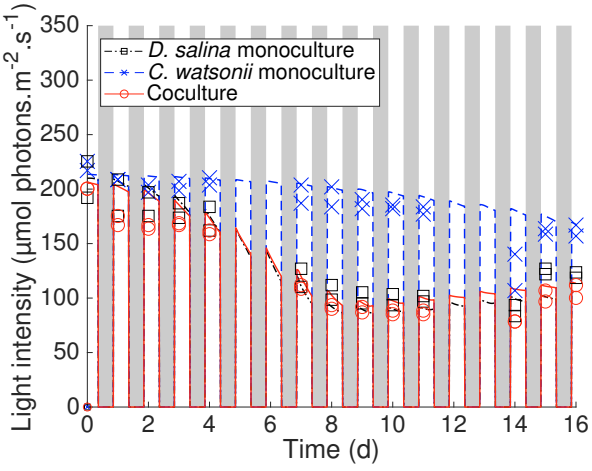


Fig. 4. Light in monocultures and cocultures (lines: theoretical data, symbols: experimental data). White and grey areas stand for daytime and nighttime, respectively.

.

Moreover, the model represents the increase of *D. salina*'s mortality when cocultivated with *C. watsonii* (Figure 1). Some cyanobacteria are known to produce cyanotoxins (Dunker et al., 2017; Zanchett and Oliveira-Filho, 2013) but nothing is known about a potential production of toxins by *C. watsonii*. The model thus supports the hypothesis that such toxin induces mortality. This allelopathic effect of *C. watsonii* on *D. salina* is well simulated by the model (Figure 1).

5. SIMULATING NITROGEN RECYCLING

5.1 Model adaptation

In this last section, we assume that a fraction of the diazotroph-derived compound P can be recycled by heterotrophic bacteria and eventually produce a source of nitrogen which can be uptaken by *D. salina*. The model was therefore modified to account for this potential (and desirable) recycling.

Equation 4 was modified to account for the consumption by bacteria. For sake of simplicity, bacteria were assumed to be at a high enough density, so that recycling rate is simply proportional to the concentration of P:

$$\frac{dP}{dt} = \alpha C - \upsilon P - \gamma P \tag{10}$$

where γ is the diazotroph-derived product uptake rate (d^{-1}).

Only a fraction β of the consumed P by bacteria is assumed to be remineralized and available for *D. salina*. The dynamics of nitrogen substrate must then be modified accordingly, by integrating this new source of nitrogen as follows:

$$\frac{dS}{dt} = -\rho_m \frac{S}{S+K_S}\left(\frac{Q_L - Q}{Q_L - Q_0}\right)D + \upsilon S_{in} - \upsilon D + \beta\gamma P \tag{11}$$

5.2 Biomass productivity of the coupled ecosystem

The performance of this microalgae-cyanobacteria-bacteria ecosystem was simulated for various dilution rates and influent nitrate S_{in}. The objective was to determine the operational conditions which enhance the production of *D. salina*, in comparison to the monoculture which does not benefit from diazotrophy.

The biomass nitrogen productivity δ was determined as the product of the dilution rate and *D. salina* cellular concentration per unit of nitrogen:

$$\delta = \frac{\upsilon D}{S_{in}} \tag{12}$$

A biomass nitrogen productivity ratio Δ was therefore calculated to determine the best case conditions for enhancing biomass nitrogen productivity from monoculture to coculture as shown in Figure 5:

$$\Delta = \frac{\delta_{coculture}}{\delta_{monoculture}} \tag{13}$$

The nitrogen use efficiency η was determined as follows:

$$\eta = \frac{QD}{S_{in}} \tag{14}$$

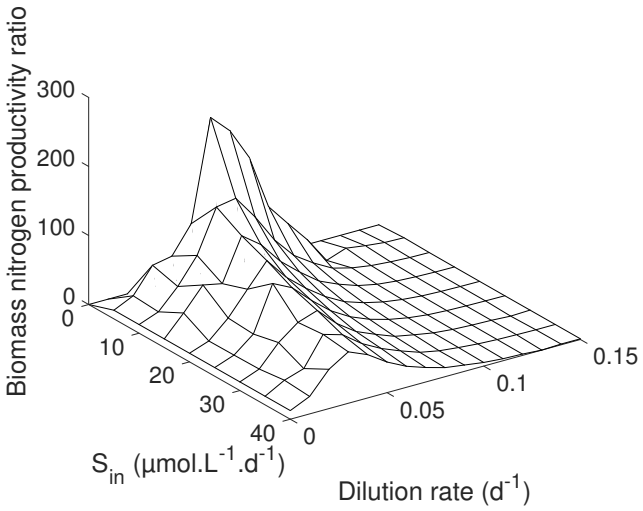


Fig. 5. *D. salina* biomass nitrogen productivity ratios

.

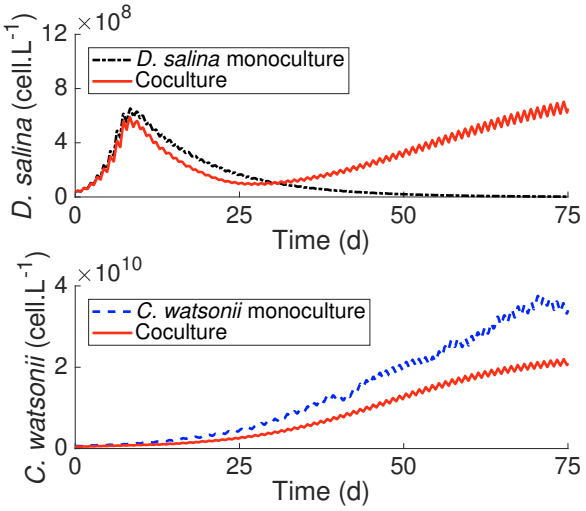


Fig. 6. *D. salina* and *C. watsonii* in monocultures and cocultures

.

In the simulated cases, biomass nitrogen productivity is better enhanced when dilution rate is 0.05 d^{-1} and influent nitrate is 5 $\mu mol.L^{-1}.d^{-1}$ (Figure 5). As a result, biomass nitrogen productivity and nitrogen use efficiency are 253 and 367 higher, respectively. Cell growths over time were therefore simulated in this case as shown in Figure 6. Nitrate addition to the coculture promotes *D. salina* growth. But then, the shading of *D. salina* penalizes *C. watsonii* (Figure 6). Finally, efficient nitrogen recycling rates are only obtained for very low *D. salina* biomass productivities.

6. CONCLUSION

This study shows that it is possible to enhance *D. salina*'s productivity when cocultivated with *C. watsonii*. This strategy can work when some bacterial communities efficiently recycle nitrogen derived from diazotrophic activity. However, the shading of *D. salina* jeopardizes *C. watsonii*

growth and eventually cancels the benefit of the coculture. To bypass this negative interaction, the two species should be cultivated in membrane-separated reactors to avoid light competition but to allow molecular exchanges. In this case, both species will no more compete for light. More works remain to be done to explore this possibility.

ACKNOWLEDGEMENTS

The authors would like to thank Sophie Marro, Sophie Rabouille, Amélie Talec and Meng Zhang for their help and comments. This work was supported by the ANR Phycover (ANR-14-CE04-0011) and the Inria Project Lab Algae in silico. M. Caia benefited from an INRA funding.

REFERENCES

Barra, L., Chandrasekaran, R., Corato, F., and Brunet, C. (2014). The challenge of ecophysiological biodiversity for biotechnological applications of marine microalgae. *Marine drugs*, 12(3), 1641–1675.

Bernard, O. (2011). Hurdles and challenges for modelling and control of microalgae for CO_2 mitigation and biofuel production. *Journal of Process Control*, 21(10), 1378–1389.

Berthelot, H., Bonnet, S., Camps, M., Grosso, O., and Moutin, T. (2015). Assessment of the dinitrogen released as ammonium and dissolved organic nitrogen by unicellular and filamentous marine diazotrophic cyanobacteria grown in culture. *Frontiers in Marine Science*, 2, 80.

Berthelot, H., Bonnet, S., Grosso, O., Cornet, V., and Barani, A. (2016). Transfer of diazotroph-derived nitrogen towards non-diazotrophic planktonic communities: a comparative study between *Trichodesmium erythraeum*, *Crocosphaera watsonii* and *Cyanothece* sp. *Biogeosciences*, 13(13), 4005–4021.

Bonnefond, H., Moelants, N., Talec, A., Bernard, O., and Sciandra, A. (2016). Concomitant effects of light and temperature diel variations on the growth rate and lipid production of *Dunaliella salina*. *Algal Research*, 14, 72–78.

Bougaran, G., Bernard, O., and Sciandra, A. (2010). Modeling continuous cultures of microalgae colimited by nitrogen and phosphorus. *Journal of theoretical biology*, 265(3), 443–454.

Do Nascimento, M., Rizza, L.S., Di Palma, A.A., de los Angeles Dublan, M., Salerno, G., Rubio, L.M., and Curatti, L. (2015). Cyanobacterial biological nitrogen fixation as a sustainable nitrogen fertilizer for the production of microalgal oil. *Algal Research*, 12, 142–148.

Dron, A., Rabouille, S., Claquin, P., Chang, P., Raimbault, V., Talec, A., and Sciandra, A. (2012). Light: dark (12: 12 h) quantification of carbohydrate fluxes in *Crocosphaera watsonii*. *Aquatic Microbial Ecology*, 68(1), 43–55.

Dunker, S., Althammer, J., Pohnert, G., and Wilhelm, C. (2017). A fateful meeting of two phytoplankton species–chemical vs. cell-cell-interactions in co-cultures of the green algae *Oocystis marsonii* and the cyanobacterium *Microcystis aeruginosa*. *Microbial ecology*, 1–11.

Fachet, M., Flassig, R.J., Rihko-Struckmann, L., and Sundmacher, K. (2014). A dynamic growth model of *Dunaliella salina*: Parameter identification and profile likelihood analysis. *Bioresource technology*, 173, 21–31.

Fouilland, E. (2012). Biodiversity as a tool for waste phycoremediation and biomass production. *Reviews in Environmental Science and Bio/Technology*, 11(1), 1–4.

Fuentes, J.L., Garbayo, I., Cuaresma, M., Montero, Z., González-del Valle, M., and Vílchez, C. (2016). Impact of microalgae-bacteria interactions on the production of algal biomass and associated compounds. *Marine drugs*, 14(5), 100.

Goebel, N.L., Edwards, C.A., Carter, B.J., Achilles, K.M., and Zehr, J.P. (2008). Growth and carbon content of three different-sized diazotrophic cyanobacteria observed in the subtropical north pacific. *Journal of Phycology*, 44(5), 1212–1220.

Grimaud, G.M., Rabouille, S., Dron, A., Sciandra, A., and Bernard, O. (2014). Modelling the dynamics of carbon–nitrogen metabolism in the unicellular diazotrophic cyanobacterium *Crocosphaera watsonii* WH8501, under variable light regimes. *Ecological modelling*, 291, 121–133.

Guillard, R.R.L. (1975). Culture of phytoplankton for feeding marine invertebrates. In M.H. Chanley and W.L. Smith (eds.), *Culture of Marine Invertebrate Animals*, 26–60. Plenum Press, New York.

Huisman, J., Jonker, R.R., Zonneveld, C., and Weissing, F.J. (1999). Competition for light between phytoplankton species: experimental tests of mechanistic theory. *Ecology*, 80(1), 211–222.

Le Chevanton, M., Garnier, M., Bougaran, G., Schreiber, N., Lukomska, E., Bérard, J.B., Fouilland, E., Bernard, O., and Cadoret, J.P. (2013). Screening and selection of growth-promoting bacteria for *Dunaliella* cultures. *Algal Research*, 2(3), 212–222.

Minowa, T. and Sawayama, S. (1999). A novel microalgal system for energy production with nitrogen cycling. *Fuel*, 78(10), 1213–1215.

Olli, K., Klais, R., and Tamminen, T. (2015). Rehabilitating the cyanobacteria–niche partitioning, resource use efficiency and phytoplankton community structure during diazotrophic cyanobacterial blooms. *Journal of Ecology*, 103(5), 1153–1164.

Pujo-Pay, M. and Raimbault, P. (1994). Improvement of the wet-oxidation procedure for simultaneous determination of particulate organic nitrogen and phosphorus collected on filters. *Marine Ecology Progress Series*, 203–207.

Ramanan, R., Kim, B.H., Cho, D.H., Oh, H.M., and Kim, H.S. (2016). Algae–bacteria interactions: evolution, ecology and emerging applications. *Biotechnology advances*, 34(1), 14–29.

Thompson, A.W., Foster, R.A., Krupke, A., Carter, B.J., Musat, N., Vaulot, D., Kuypers, M.M., and Zehr, J.P. (2012). Unicellular cyanobacterium symbiotic with a single-celled eukaryotic alga. *Science*, 337(6101), 1546–1550.

Ying, K., Zimmerman, W., and Gilmour, D. (2014). Effects of CO_2 and pH on growth of the microalga *Dunaliella salina*. *Journal of Microbial and Biochemical Technology*, 6(3), 167–173.

Zanchett, G. and Oliveira-Filho, E.C. (2013). Cyanobacteria and cyanotoxins: from impacts on aquatic ecosystems and human health to anticarcinogenic effects. *Toxins*, 5(10), 1896–1917.